

Antitumor Agents. 2. Synthesis, Structure–Activity Relationships, and Biological Evaluation of Substituted 5*H*-Pyridophenoxazin-5-ones with Potent Antiproliferative Activity

Adele Bolognese,^{*,†} Gaetano Correale,[†] Michele Manfra,[†] Antonio Lavecchia,[§] Orazio Mazzoni,[§] Ettore Novellino,[§] Vincenzo Barone,[‡] Paolo La Colla,^{||} and Roberta Loddo^{||}

Dipartimento di Chimica Organica e Biochimica and Dipartimento di Chimica, Università di Napoli "Federico II", Via Cynthia 6, Monte Sant'Angelo, I-80126 Napoli, Italy, Dipartimento di Chimica Farmaceutica e Tossicologica, Università di Napoli "Federico II", Via D. Montesano 49, 80131 Napoli, Italy, and Dipartimento di Biologia Sperimentale, Sezione di Microbiologia, Università di Cagliari, Cittadella Universitaria SS 554, I-09042 Monserrato (Cagliari), Italy

Received April 23, 2002

New antiproliferative compounds, 5*H*-pyrido[3,2-*a*]phenoxazin-5-ones (**1–10**), 5*H*-benzophenoxazin-5-one (**11**), 5*H*-pyrido[2,3-*a*]phenoxazin-5-one (**12**), 5*H*-pyrido[3,4-*a*]phenoxazin-5-one (**13**), and 5*H*-pyrido[4,3-*a*]phenoxazin-5-one (**14**), were synthesized and evaluated against representative human neoplastic cell lines. The excellent cytotoxic activity of these polycyclic phenoxazinones, structurally related to the actinomycin chromophore, is discussed in terms of structural changes made to rings A and D (Chart 1). Electron-withdrawing or electron-donating substituents were introduced at different positions of ring A to probe the electronic and positional effects of the substitution. A nitro group in R₂ or in R₁ increases the cytotoxic activity, whereas electron-donating methyl groups in any position lead to 10- to 100-fold decreasing of the activity. The low antiproliferative activity of benzophenoxazinone **11** and pyridophenoxazinones **13** and **14** confirms the crucial role of pyridine nitrogen in the W position of ring D in DNA binding. The unexpected high activity exhibited by **12**, which has the nitrogen in the X position, could be ascribed to a different mechanism of action, which needs further investigation.

Introduction

The quinonic nucleus is common to many natural and synthetic products associated with anticancer and antibacterial activities.¹ These compounds are typically DNA-intercalating agents because of the ability of their large, planar polycycles to bind strongly between the base pairs through hydrogen bonds and π -stacking interactions.^{2,3} They usually have side chains or sugar substituents and basic nitrogens, which upon protonation further strengthen the DNA binding. Examples of quinone derivatives with antitumor activity include mitoxantrone,⁴ doxorubicin,⁴ mitomycin,⁵ streptonigrin,⁶ and actinomycin D (AMD).² All known quinonic DNA intercalators have the potential to disrupt the normal function of DNA, leading to cell death.⁷ This DNA damage can be caused either by the parent form or by its metabolic conversion to electrophilic or radical species.⁸

In a recent paper,⁹ we described a potent anticancer synthetic iminoquinone, the 5*H*-pyrido[3,2-*a*]phenoxazin-5-one (PPH), able to inhibit a large number of lymphoblastoid and solid-tumor-derived cells at submicromolar concentrations (Chart 1).

Interestingly, this compound also exhibits high inhibitory activity on the proliferation of wild-type and

multidrug-resistant KB cells. In fact, "multidrug resistance" (MDR), a phenomenon due to the prolonged use of chemotherapeutic agents, currently constitutes the major problem in cancer treatment. From these studies, we concluded that the excellent cytotoxic activity of PPH results from the intercalation at the middle 5'-GC-3' base pairs of the octamer [d(GAAGCTTC)]₂.⁹ Two strong hydrogen bonds were observed between the hydrogen of the charged pyridine nitrogen and both (i) the O4' in the deoxyribose ring of the cytosine C5 residue and (ii) the O5' of the phosphate backbone located between the G4 and C5 residues. Additional stability of the complex arises from π - π stacking interactions between the tetracyclic pyridophenoxazinone system and the aromatic base rings.

In light of these results, we examined structure–activity relationships (SARs), using PPH as lead compound and assessing the effects on biological activity of structural changes made to rings A and D. In the new series of compounds, the influence on antiproliferative activity of electron-withdrawing and -donating substituents at different positions of the benzene ring A (compounds **1–10**) was investigated first (Chart 1). Subsequently, the influence of the nitrogen position within the pyridine fused ring D (compounds **12–14**) was analyzed. Finally, 5*H*-benzo[*a*]phenoxazin-5-one¹⁰ (**11**) was synthesized and evaluated to confirm the crucial role played by the pyridine moiety in the cytotoxic activity. The present paper describes the synthesis and assessment of the *in vitro* antitumor activity of these substances.

* To whom correspondence should be addressed. Phone: ++39 081 674121. Fax: ++39 081 674393. E-mail: bologne@unina.it.

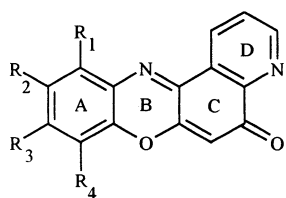
[†] Dipartimento di Chimica Organica e Biochimica, Università di Napoli "Federico II".

[§] Dipartimento di Chimica Farmaceutica e Tossicologica, Università di Napoli "Federico II".

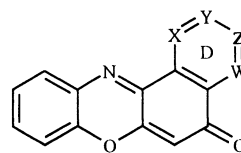
[‡] Dipartimento di Chimica, Università di Napoli "Federico II".

^{||} Università di Cagliari.

Chart 1



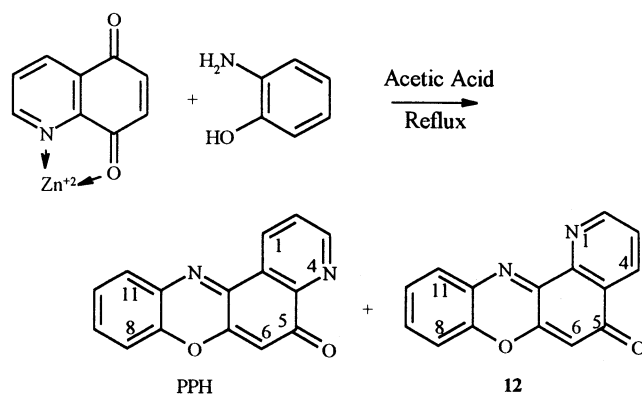
Compd	R ₁	R ₂	R ₃	R ₄
1	NO ₂	H	H	H
2	H	NO ₂	H	H
3	H	H	NO ₂	H
4	H	H	H	NO ₂
5 ^a	H	Cl	H	H
6	H	CN	H	H
7	CH ₃	H	H	H
8 ^a	H	CH ₃	H	H
9	H	H	CH ₃	H
10	H	H	H	CH ₃
PPH ^a	H	H	H	H



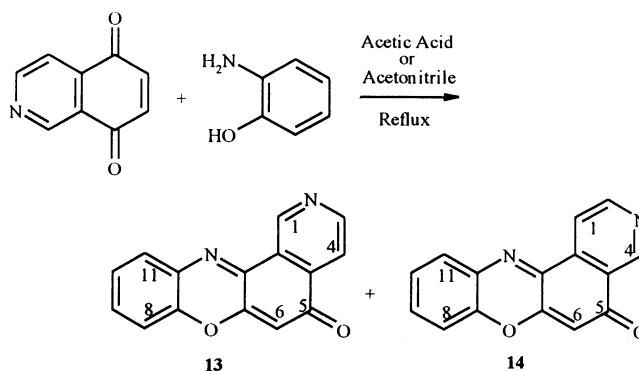
Compd	X	Y	Z	W
11 ^b	CH	CH	CH	CH
12 ^a	N	CH	CH	CH
13	CH	N	CH	CH
14	CH	CH	N	CH

^a Compounds **5**, **8**, **12**, and PPH are described in ref 11. ^b Compound **11** is described in ref 10.

Scheme 1



Scheme 2



Results and Discussion

Chemistry. Condensation of 2-aminophenol and quinolin-5,8-dione in acetic acid, assisted by a Zn(II)/quinolin-5,6-dione complex, has been reported to yield PPH in good amounts.⁹ PPH derivatives (**1–12**) were prepared according to this previously reported general procedure using the substituted 2-aminophenols and quinolin-5,8-dione as starting products (Scheme 1).

To prepare the 5*H*-pyrido[3,4-*a*]phenoxazin-5-one (**13**) and the 5*H*-pyrido[4,3-*a*]phenoxazin-5-one (**14**), isoquinolin-5,8-dione was synthesized by hydroxylation and oxidation of 5-hydroxyisoquinoline with [bis(trifluoroacetoxy)]iodobenzene in acetonitrile/water.¹² Isoquinolin-5,8-dione and 2-aminophenol were refluxed for 2 h in acetic acid or acetonitrile, a protic or nonprotic

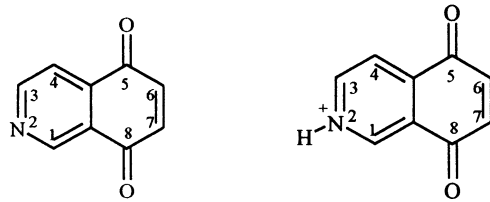
Table 1. Yields of the Reaction between Isoquinolin-5,8-dione (1 mmol) and 2-Aminophenol (1 mmol) in Acetic Acid and Acetonitrile

solvent	reaction yield, %	
	13 + 14	13/14
acetic acid	42	1:3
acetonitrile	30	1:1.2

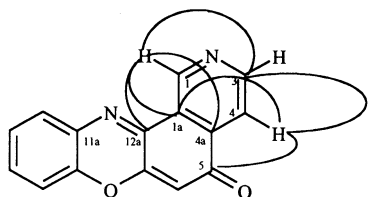
solvent, respectively (Scheme 2). Table 1 reports the reaction yields.

Apparently, compounds **13** and **14** seem to arise from a nucleophilic attack of the amino group of 2-aminophenol on the 5 and 8 carbonyl carbons of the isoquinolin-5,8-dione. With this point of view, equal amounts of **13** and **14** would be expected.

The net atomic charges computed for the isoquinolin-5,8-dione system rule out the possibility of a leading role

Table 2. HOMO and LUMO Orbital Coefficients and Charge Density of Nonprotonated and N-Protonated Quinolin-5,8-dione Calculated by Quantum Mechanical Methods


	orbital coefficient, nonprotonated (eV)			orbital coefficient, N-protonated (eV)		
	HOMO	LUMO	net atomic charge (e ⁻)	HOMO	LUMO	net atomic charge (e ⁻)
C ₅	-0.1082	-0.2985	0.4249	-0.1562	-0.1689	0.4333
C ₈	-0.1694	0.2884	0.4149	-0.1662	0.0995	0.4483
C ₆	0.2405	-0.3270	0.0141	0.5254	-0.0819	0.0780
C ₇	0.2221	0.3351	0.0183	0.5208	0.1337	0.0751

**Figure 1.** Structural assignment of **13**, showing HMBC relationships of H1 and H4.

of the electrostatic interactions in determining the preferred site of attack and do not explain the different yields of **13** and **14** in protic and nonprotic media. Therefore, an orbital interaction between the nucleophilic amino group of the 2-aminophenol and the α,β -unsaturated system of the isoquinolin-5,8-dione was hypothesized, according to the frontier orbital theory.¹³ Table 2 reports the Mulliken atomic charges together with the HOMO (highest occupied molecular orbital) and LUMO (lowest unoccupied molecular orbital) coefficients of neutral and N-protonated isoquinolin-5,8-dione.

In acetonitrile, the LUMO coefficients of the nonprotonated α,β -unsaturated system decrease (absolute value) in the order $7 > 6 > 5 > 8$, while in acetic acid, they decrease in the order $5 > 7 > 8 > 6$. In the reaction between 2-aminophenol and isoquinolin-5,8-dione in acetic acid, the formation of **14** is favored by the amino group attack on the carbon at the 5 position. In contrast, in nonprotic medium, carbon 7, which has the largest coefficient, undergoes nucleophilic attack by the amino group of 2-aminophenol. In this way, compound **13** is formed via hemiketal according to the reaction previously reported.⁹ The multistep pathway is responsible for the low yield.

The Experimental Section reports general synthetic procedures and characterization of all new compounds on the basis of spectral data and by elemental analysis. Structural assignment of **13** and **14** was accomplished through extensive 2D NMR spectroscopy, HMQC, and HMBC. The relationships of **13** are reported in Figure 1. In the HMBC spectra of **13**, the singlet assigned to the more deshielded H1 proton at δ_{H} 9.92 shows a very significant, strong correlation with the singlets at δ_{C} 146.0 (C12a), 137.0 (C4a), and 124.9 (C1a) and with the doublet at δ_{C} 152.4 (C3). Moreover, the H4 doublet at δ_{H} 8.02 shows correlation with the singlets at δ_{C} 182.4 (C5) and 124.9 (C1a) and with the doublet at δ_{C} 152.4 (C3).

Antiproliferative Activity. The antiproliferative activity of the PPH derivatives **1–10** and analogues **11–14** was evaluated against a panel of 15 human cell lines representative of liquid and solid human tumors, and the results are shown in Table 3. Data for the anticancer agents PPH, doxorubicin, and AMD are included for comparison.

SAR studies based on PPH were designed to assess the effects on cytotoxic activity of structural changes made to the benzo- and pyrido-fused rings A and D.

Structure–Activity Relationships (SARs) of Ring A Substituents. Since π - π stacking interactions play a role in the binding of these compounds to DNA,

Table 3. Antitumor Activity of 1-14 and PPH Compared to Doxorubicin and Actinomycin D

cell lines	IC ₅₀ ^a (μM)														PPH ⁹	doxo	AMD
	1	2	3	4	5	6	7	8	9	10	11	12	13	14			
leukemia/lymphoma																	
Wil2-NS	0.05	0.001	0.70	0.10	0.06	0.06	0.08	0.10	0.06	0.20	19.00	0.50	20.10	17.90	0.05	0.02	0.003
Raji	0.02	0.15	0.90	1.00	0.1	2.4	5.70	2.10	2.80	0.40	>50	3.80	9.60	9.60	0.04	0.03	0.002
MOLT-4	0.008	0.004	0.10	0.06	0.05	0.02	0.70	0.08	0.10	0.30	10.00	2.00	8.00	5.00	0.04	0.02	0.001
C8166	0.005	0.10	0.03	0.10	0.04	0.1	0.30	0.20	0.10	0.60	>50	4.70	7.15	4.80	0.10	0.02	0.0008
MT-4	0.02	0.01	0.20	0.09	0.03	0.03	0.04	0.07	0.03	0.05	>50	0.70	3.50	4.50	0.01	0.01	0.0009
CCRF-SB	0.002	0.002	0.30	0.04	0.06	0.05	0.04	0.05	0.08	0.04	3.60	1.50	3.50	2.70	0.009	0.02	0.001
CCRF-CEM	0.01	0.007	0.30	0.05	0.01	0.02	0.80	0.25	0.10	0.07	>50	1.50	18.00	22.00	0.01	0.03	0.003
carcinoma																	
G-361	0.01	0.05	0.60	0.20	0.1	0.05	0.78	0.30	0.10	0.40	>50	0.50	35.00	10.70	0.01	0.09	0.001
MCF-7	0.30	0.01	0.30	0.50	0.6	0.01	0.50	0.60	0.70	1.20	3.20	0.065	20.03	15.20	0.23	0.05	0.006
HepG-2	0.90	0.60	0.50	0.90	0.9	0.04	0.70	0.30	0.70	0.90	5.20	0.11	13.80	16.00	0.05	0.12	0.010
ACHN	0.05	0.001	0.40	0.08	0.03	0.02	0.05	0.08	0.03	0.07	3.60	0.60	10.00	23.10	0.01	0.04	0.005
5637	0.06	0.003	0.50	0.10	0.07	0.04	0.10	0.09	0.05	0.20	5.00	0.90	17.50	19.02	0.01	0.02	0.003
HT-29	1.20	0.20	1.50	2.20	0.6	1.9	1.20	1.50	0.50	1.90	>50	0.50	16.00	18.10	0.25	0.15	0.006
HeLa	0.08	0.30	1.40	0.50	0.1	0.04	0.12	0.20	0.10	0.10	8.20	2.70	5.60	7.70	0.20	0.07	0.04
Hep-2	0.05	0.40	1.10	0.70	0.2	0.02	0.60	0.30	0.20	0.20	1.40	1.20	7.90	8.90	0.04	0.04	0.004

^a Compound concentration required to reduce cell proliferation by 50%, as determined the MTT method, under conditions allowing untreated controls to undergo at least three consecutive rounds of multiplication. Data represent mean values for three independent determinations. Wil2-NS, human splenic B-lymphoblastoid cells; Raji, human Burkitt lymphoma; MOLT-4, human acute T-lymphoblastic leukemia; C8166 and MT-4, CD4⁺ human acute T-lymphoblastic leukemia; CCRF-CEM, human acute T-lymphoblastic leukemia; CCRF-SB, human acute B-lymphoblastic leukemia; SKMEL-28 and G361, human skin melanoma; MCF-7, human breast adenocarcinoma; HepG-2, human hepatocellular carcinoma; ACHN, human renal adenocarcinoma; 5637, human bladder carcinoma; HT-29, human colon adenocarcinoma; HeLa, cervix carcinoma; Hep-2, larynx carcinoma; IMR-32, human neuroblastoma; CRL-7065, human foreskin fibroblasts.

Table 4. HOMO and LUMO Energies of Cytosine, Guanine, **2**, **5**, **6**, and PPH and LUMO Coefficients of the Carbon in the 11a Position Calculated by Quantum Mechanical Methods

	guanine	cytosine	2	5	6	PPH
HOMO (eV)	-6.2919	-6.8470	-7.2609	-6.8024	-7.1490	-6.7017
LUMO (eV)	-0.4890	-1.1083	-3.6189	-3.3500	-3.5721	-3.1748
LUMO _{C11a} coefficient			0.1614	0.1603	0.1534	0.1359

according to the results reported in a previous paper,⁹ we prepared derivatives substituting the benzene ring A with electron-withdrawing (**1–6**) and electron-donating groups (**7–10**).

From the median of the IC₅₀ values for each compound across the 15 human tumor cell lines, **2** with a nitro group appended to the 2-position of ring A was seen to be the most cytotoxic compound with a median value of 0.01 μ M (Table 3). This compound showed higher cytotoxic potency against the lymphoblastoid cell lines Wil2-NS (IC₅₀ = 0.001 μ M), MOLT-4 (IC₅₀ = 0.004 μ M), CCRF-SB (IC₅₀ = 0.002 μ M), and CCRF-CEM (IC₅₀ = 0.007 μ M) than PPH. Among the solid-human tumors, ACHN and 5637 cells were more prone to the antiproliferative effect of **2** (IC₅₀ = 0.001 and 0.003 μ M, respectively).

Compound **1**, substituted with a nitro group in the 1-position and more cytotoxic against MOLT-4 (IC₅₀ = 0.008 μ M), C8166 (IC₅₀ = 0.005 μ M), and CCRF-SB cells (IC₅₀ = 0.002 μ M), was almost equipotent to PPH. The presence of a nitro group in the 4- and 3-positions resulted in a 10- to 50-fold decrease in potency (compare **4** and **3** vs **2** and PPH).

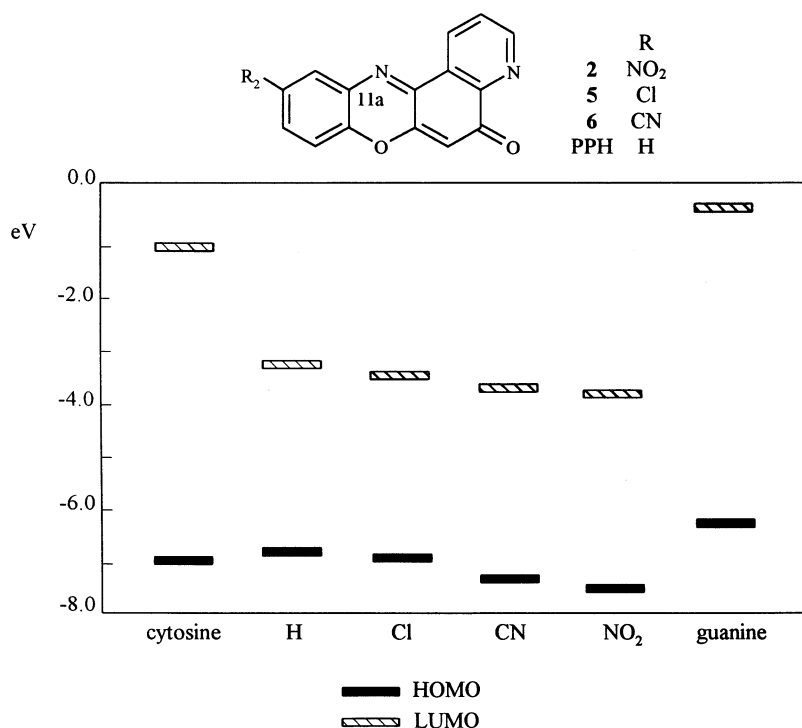
Since the electron-withdrawing nitro group in the 2-position of ring A provided the best cytotoxicity, derivatives **5** and **6** with chloro and cyano groups in the 2-position were synthesized, evaluated for their antiproliferative activity, and found to be very active

(median IC₅₀ = 0.07 and 0.04 μ M, respectively). In conclusion, the nitro group in the 2-position seems to provide a better effect than chloro and cyano groups.

Next, we examined the influence of the electron-donating methyl substituent on ring A. The data collected in Table 3 show that the methyl derivatives **7–10** were less active than PPH, with a median IC₅₀ value ranging between 0.1 and 0.50 μ M, and were 1–2 orders of magnitude less potent than the corresponding nitro, chloro, and cyano derivatives **1–6**.

Since no significant steric clashes were observed between the substituents of the pyridophenoxazinones **1–10** and the DNA sugar–phosphate backbone at the PPH intercalation site, the difference in potency of these compounds could be ascribed to electronic effects. In fact, substitution by the electron-withdrawing groups produces an electron-deficient ring A, which in turn can improve stacking interactions with purine and pyrimidine bases in the DNA active site (GC–CG of opposite strands). In contrast, the electron-donating methyl groups, enriching ring A with electron density, weaken the stacking interactions.

To support this hypothesis, frontier molecular orbital energies and atomic orbital coefficients were calculated by ab initio methods,^{14–18} both for the pyridophenoxazinones PPH, **2**, **5**, and **6** and for the guanine and cytosine bases, which were hypothesized to be the principal counterparts in the binding site (Table 4). As is well-known,¹³ the energies of HOMO and LUMO are respectively a rough measure of the electron-donating and electron-acceptor ability of a molecule. Our results show that the HOMO–LUMO gap between the guanine and cytosine electron donors and the pyridophenoxazinones electron acceptors decreases according to substituent R₂ in the order NO₂ < CN < Cl < H (Figure 2). As illustrated in Table 4, the LUMO coefficient of the

**Figure 2.** Diagram of HOMO–LUMO energies (eV) of cytosine and guanine bases and pyridophenoxazinones **2**, **5**, **6**, and PPH calculated at the PBE0 6-31G(d,p) level.

carbon at the 11a-position, peculiarly involved in the π - π interactions,⁹ also increases in PPH, **2**, **5**, and **6** according to the order NO₂ > CN > Cl > H. Consequently, the LUMO energy of the pyridophenoxazinones and the atomic orbital coefficients of C11a contribute to make the nitro derivative **2** the most active compound.

SAR of Nitrogen Position within Ring D. Molecular modeling studies⁹ suggested that two strong hydrogen bonds stabilize the PPH/DNA complex involving the hydrogen of the positively charged pyridine nitrogen of the ligand and the negatively charged oxygen atoms (O4' and O5') of the cytosine C5 residue. Therefore, to confirm the crucial role of pyridine nitrogen, benzophenoxazinone **11** and pyridophenoxazinones **12**–**14**, where the nitrogen atom occupies the X, Y, and Z positions (Chart 1), were synthesized and evaluated for their antiproliferative activity.

Comparison of the activities of compounds **12**–**14** revealed that **13** and **14**, bearing the pyridine nitrogen in the Y and Z positions, show low antiproliferative activity, whereas compound **12** with nitrogen at the X position demonstrates the highest potency across the panel of lymphoblastoid and carcinoma cell lines, with a median IC₅₀ value of 0.90 μ M. A significant inhibitory effect of **12** was observed on the proliferation of the solid-human-tumor-derived cell lines, with the lowest IC₅₀ values for MCF-7 (IC₅₀ = 0.065 μ M), G361 (IC₅₀ = 0.50 μ M), HT-29 (IC₅₀ = 0.50 μ M), and ACHN (IC₅₀ = 0.60 μ M). The lymphoblastoid cells Wil2-NS and MT-4 were also very sensitive (IC₅₀ = 0.50 and 0.70 μ M, respectively).

The benzophenoxazinone **11** exhibited limited cytotoxicity in most of the cell lines, confirming the significant role of the pyridine nitrogen in the DNA recognition process.

The unexpected high antiproliferative activity exhibited by **12**, which does not have the pyridine nitrogen in a suitable position to engage a hydrogen bond as in PPH, could be ascribed to a different binding mode. In fact, the intercalation process represents only one of many events participating in the inhibition of cellular proliferation (i.e., the formation of complexes between DNA and topoisomerases or transition metals and DNA-cleaving radicals, etc.). Particularly, compound **12** could act also like a metal chelating agent. In fact, a number of papers report that metal ions play an important role in altering the biochemical properties of antibiotics containing a quinone chromophore.¹⁹ Metal coordination, altering the charge distribution across the molecules, affects the redox potential of the quinone and hence directly influences the rate of generation of DNA-damaging radical species.

Conclusions

In this study, we report a series of 5*H*-pyridophenoxazin-5-ones (**1**–**14**), derivatives and analogues of PPH, exhibiting activity against leukemia and solid tumor cell lines at submicromolar concentrations. The nitro derivative **2** was the most cytotoxic compound with an IC₅₀ median value of 0.01 μ M, and its high activity is in agreement with a theoretical investigation on the electron-withdrawing effect of the nitro group on the π - π -stacking interactions. The effects of substitution

on the benzo-fused ring A and of the nitrogen position within the pyrido-fused ring D were investigated. Two important features seem to contribute to the cytotoxic activity of these anticancer DNA ligands: (i) the presence of electron-withdrawing substituents on ring A, particularly at R₂ and R₁, and (ii) the pyridine nitrogen in the X and W positions of ring D (Chart 1).

Whether the antitumor activities of this class of compounds that we synthesized are exerted through DNA intercalative binding and/or through other mechanisms is not yet known. However, it has been shown²⁰ that the phenoxazinone ring system of the DNA intercalating AMD undergoes enzymatic single-electron reduction to a free radical intermediate. Transfer of the electron to the oxygen, yielding the superoxide, can cause intracellular macromolecular damage and cell death. These results could account for the cytotoxic activity of pyridophenoxazinones **1**–**14**, which possess an iminoquinone function capable of involving a one-electron redox reaction. Compounds **1**–**6**, having electron-withdrawing substituents on phenoxazinone ring A, could be structurally more prone to single-electron reduction to the free radical state. In fact, the capacity of quinones to accept electrons is due to the electron-attracting or -donating substituents that modulate the redox properties responsible for the oxidative stress. Moreover, the high antiproliferative activity of phenoxazinones **1**–**4**, containing an additional nitro reduction site, could also be imputed to the formation of cellular-damaging reactive amine species. Compound **12**, with nitrogen at the X position, exhibits an unexpectedly high cytotoxicity (median IC₅₀ = 0.90 μ M), suggesting a binding mode different from PPH. This compound could be expected to act as a metal chelating agent. Experiments are under way to characterize the mechanisms of action of these drugs.

From a synthetic point of view, accessibility of this class of compounds has required the use of a metal-assisted methodology. The results presented here also report a mechanistic study of the reaction among quinolin-5,8-dione, isoquinolin-5,8-dione, and 2-aminophenol.

Experimental Section

Chemistry. Melting points were determined by a Kofler apparatus and are uncorrected. The elemental analysis (C, H, and N) of reported compounds agrees with the calculated values and was within $\pm 0.4\%$ of theoretical values. Electron impact (EI) mass spectra were obtained at 70 eV on a ZAB 2F spectrometer. The purity of compounds was checked by ascending TLC on Merck's silica gel plates (0.25 mm) with fluorescent baking. The IR spectra were recorded on a Perkin-Elmer 399 spectrometer in KBr. The C=O and C=N stretches lie between 1628 and 1635 cm⁻¹. NMR measurements (data reported in δ) were performed on a Bruker AMX-500 spectrometer equipped with a Bruker X-32 computer, using the UYNMR software package. NMR spectra were measured at 500 MHz (¹H) and 125 MHz (¹³C). The chemical shifts are referenced to ¹³CDCl₃ and CDCl₃ solvent signals at 77.0 and 7.26 ppm, respectively. Standard pulse sequences were employed for magnitude COSY. HMQC and HMBC experiments were optimized for ¹J_{C-H}=135 Hz and ^{2,3}J_{C-H}=10 Hz, respectively. Me₄Si was used as an internal reference.

Substituted 5*H*-Pyrido[3,2-*a*]phenoxazin-5-ones (1**–**10**).** Substituted 2-aminophenols (0.01 mol) in methanol/acetic acid (50:50 v/v, 10 mL) were added dropwise to an equimolar mixture of 5,8-quinolinquinone (0.01 mol) and Zn(II) acetate

(0.01 mol) in acetic acid (50 mL), and the mixture was stirred and gently warmed until the dark color showed complex formation. The reaction mixture, refluxed for 2 h, was evaporated in vacuo and acidified (6 N HCl) to break the Zn complex and was extracted by chloroform. The organic layer, evaporated in vacuo and purified on a silica gel column, afforded pyridophenoxazinones **1–10** as main products, which were crystallized (EtOAc).

11-Nitro-5H-pyrido[3,2-a]phenoxazin-5-one (1). Mp > 300 °C. UV (CHCl₃) λ_{max}, nm (log ε): 430 (3.63). ¹H NMR (CDCl₃) 9.21 (1H, d, *J* = 4.5 Hz), 9.00 (1H, d, *J* = 2.6 Hz), 8.47 (1H, d, *J* = 7.9 Hz), 8.29 (1H, dd, *J* = 2.6, 9.0 Hz), 6.68 (1H, dd, *J* = 4.5, 7.9 Hz), 7.38 (1H, d, *J* = 9.0 Hz), 6.69 (1H, s). MS *m/z*: 293 (M⁺). Anal. (C₁₅H₇N₃O₄) C, H, N.

10-Nitro-5H-pyrido[3,2-a]phenoxazin-5-one (2). Mp 295–6 °C. UV (CHCl₃) λ_{max}, nm (log ε): 413 (3.82). ¹H NMR (CDCl₃) 9.15 (1H, d, *J* = 4.0 Hz), 9.06 (1H, d, *J* = 8.1 Hz), 8.74 (1H, d, *J* = 2.6 Hz), 8.41 (1H, dd, *J* = 2.6, 9.0 Hz), 7.79 (1H, dd, *J* = 4.0, 8.1 Hz), 7.48 (1H, d, *J* = 9.0 Hz), 6.71 (1H, s). MS *m/z*: 293 (M⁺). Anal. (C₁₅H₇N₃O₄) C, H, N.

9-Nitro-5H-pyrido[3,2-a]phenoxazin-5-one (3). Mp 314–5 °C. UV (CHCl₃) λ_{max}, nm (log ε): 430 (3.16), 441 (3.17). ¹H NMR (CDCl₃) 9.15 (1H, d, *J* = 4.0 Hz), 9.06 (1H, d, *J* = 8.0 Hz), 8.24 (1H, d, *J* = 8.7 Hz), 8.22 (1H, s), 8.01 (1H, d, *J* = 8.5 Hz), 7.79 (1H, dd, *J* = 4.0, 8.0 Hz), 6.71 (1H, s). MS *m/z*: 293 (M⁺). Anal. (C₁₅H₇N₃O₄) C, H, N.

8-Nitro-5H-pyrido[3,2-a]phenoxazin-5-one (4). Mp 327–8 °C. UV (CHCl₃) λ_{max}, nm (log ε): 428 (3.58). ¹H NMR (CDCl₃) 9.30 (1H, d, *J* = 4.0 Hz), 8.98 (1H, d, *J* = 8.0 Hz), 8.20 (1H, d, *J* = 8.7 Hz), 8.10 (1H, d, *J* = 8.7 Hz), 8.01 (1H, t, *J* = 8.5 Hz), 7.75 (1H, dd, *J* = 4.0, 8.0 Hz), 6.05 (1H, s). MS *m/z*: 293 (M⁺). Anal. (C₁₅H₇N₃O₄) C, H, N.

10-Cyano-5H-pyrido[3,2-a]phenoxazin-5-one (6). Mp 245–6 °C. UV (CHCl₃) λ_{max}, nm (log ε): 418 (4.12). ¹H NMR (CDCl₃) 9.14 (1H, d, *J* = 5.4 Hz), 9.03 (1H, d, *J* = 6.9 Hz), 8.16 (1H, d, *J* = 3.1), 7.79 (1H, dd, *J* = 6.9, 3.1), 7.78 (1H, dd, *J* = 5.4, 6.9), 7.75 (1H, d, *J* = 6.9 Hz), 6.57 (1H, s). MS *m/z*: 273 (M⁺). Anal. (C₁₆H₇N₃O₂) C, H, N.

11-Methyl-5H-pyrido[3,2-a]phenoxazin-5-one (7). Mp 278–9 °C. UV (CHCl₃) λ_{max}, nm (log ε): 432 (4.30), 438 (4.32). ¹H NMR (CDCl₃) 9.08 (1H, d, *J* = 4.2 Hz), 9.05 (1H, d, *J* = 7.8 Hz), 7.71 (1H, dd, *J* = 3.2, 7.8 Hz), 7.40 (1H, t, *J* = 7.8 Hz), 7.23 (1H, d, *J* = 7.3 Hz), 7.17 (1H, d, *J* = 8.1 Hz), 6.61 (1H, s), 2.74 (3H, s). MS *m/z*: 262 (M⁺). Anal. (C₁₆H₁₀N₂O₂) C, H, N.

9-Methyl-5H-pyrido[3,2-a]phenoxazin-5-one (9). Mp 232–3 °C. UV (CHCl₃) λ_{max}, nm (log ε): 434 (3.72). ¹H NMR (CDCl₃) 9.00 (1H, d, *J* = 4.2 Hz), 8.94 (1H, d, *J* = 7.8 Hz), 7.64 (2H, m), 7.13 (1H, d, *J* = 7.8 Hz), 7.06 (1H, s), 6.51 (1H, s), 2.43 (3H, s). MS *m/z*: 262 (M⁺). Anal. (C₁₆H₁₀N₂O₂) C, H, N.

8-Methyl-5H-pyrido[3,2-a]phenoxazin-5-one (10). Mp 284–5 °C. UV λ_{max}, nm (log ε): 364.8 (3.66), 455.6 (3.64). ¹H NMR (CDCl₃) 9.10 (1H, d, *J* = 5.4 Hz), 9.07 (1H, d, *J* = 6.9 Hz), 7.72 (1H, dd, *J* = 5.4, 6.9), 7.71 (1H, dd, *J* = 6.9, 3.0), 7.41 (1H, dd, *J* = 6.9, 3.0), 7.30 (1H, t, *J* = 6.9 Hz), 6.66 (1H, s), 2.50 (3H, s). MS *m/z*: 262 (M⁺). Anal. (C₁₆H₁₀N₂O₂) C, H, N.

5H-Pyrido[3,4-a]phenoxazin-5-one (13) and 5H-Pyrido[4,3-a]phenoxazin-5-one (14). 2-Aminophenol (0.01 mol) in acetic acid or acetonitrile (50 mL) was added dropwise to a solution of 5,8-isoquinolinquinone (0.01 mol) in acetic acid or acetonitrile (20 mL). The reaction mixture, refluxed for 2 h, evaporated in vacuo, dissolved in CHCl₃, purified on a silica gel column, afforded pyridophenoxazinones **13** and **14**, which were crystallized (EtOAc).

5H-Pyrido[3,4-a]phenoxazin-5-one (13). Mp 219–20 °C. UV λ_{max}, nm (log ε): 366.4 (4.36), 450.4 (3.28). ¹H NMR (CDCl₃) 9.92 (1H, s), 8.94 (1H, d, *J* = 5.5 Hz), 8.02 (1H, d, *J* = 5.5 Hz), 7.84 (1H, d, *J* = 8.2), 7.49 (1H, t, *J* = 7.7), 7.35 (1H, t, *J* = 7.7), 7.30 (1H, d, *J* = 8.2 Hz), 6.46 (1H, s). ¹³C NMR (CDCl₃) 182.4 (s), 152.4 (d), 151.2 (s), 147.6 (d), 146.0 (s), 143.9 (s), 137.0 (s), 132.7 (s), 132.3 (d), 130.2 (d), 125.7 (d), 124.9 (s), 118.1 (d), 116.1 (d), 107.9 (d). MS *m/z*: 248 (M⁺). Anal. (C₁₅H₈N₂O₂) C, H, N.

5H-Pyrido[4,3-a]phenoxazin-5-one (14). Mp 219–20 °C. UV λ_{max}, nm (log ε): 366.4 (4.36), 450.4 (3.28). ¹H NMR (CDCl₃) 9.47 (1H, s), 8.97 (1H, d, *J* = 5.5 Hz), 8.42 (1H, d, *J* = 5.5 Hz), 7.81 (1H, d, *J* = 8.2), 7.50 (1H, t, *J* = 7.7), 7.34 (1H, t, *J* = 7.7), 7.28 (1H, d, *J* = 8.2 Hz), 6.38 (1H, s). ¹³C NMR (CDCl₃) 182.3 (s), 152.5 (d), 150.2 (s), 149.2 (d), 146.3 (s), 144.2 (s), 137.5 (s), 133.3 (d), 132.8 (s), 130.5 (d), 127.2 (s), 125.7 (d), 117.3 (d), 116.1 (d), 107.7 (d). MS *m/z*: 248 (M⁺). Anal. (C₁₅H₈N₂O₂) C, H, N.

Ab Initio Calculations. All the computations have been performed with a modified version of the Gaussian 98 package.¹⁴ The geometries of quinonoid compounds have been fully optimized by the PBE0¹⁵ density functional using the 6-31G-(d,p)¹⁶ basis set.¹⁷ The reliability of this procedure is documented in a number of recent studies.^{15,17,18} Atomic charges have been obtained at the same level using a Mulliken population analysis, whereas HOMO and LUMO coefficients have been computed at the HF/STO-3G level using the same geometries.

Biology. Compounds. Test compounds were dissolved in DMSO at an initial concentration of 200 μM and then were serially diluted in culture medium.

Cells. Cell lines were from American Type Culture Collection (ATCC). Leukemia- and lymphoma-derived cells were grown in RPMI 1640 containing 10% fetal calf serum (FCS), 100 U/mL penicillin G, and 100 μg/mL streptomycin. Solid-tumor-derived cells were grown in their specific media supplemented with 10% FCS and antibiotics. Cell cultures were incubated at 37 °C in a humidified 5% CO₂ atmosphere. Cell cultures were checked periodically for the absence of mycoplasma contamination by the Hoechst staining method.

Antiproliferative Assays. Exponentially growing leukemia and lymphoma cells were resuspended at a density of 1 × 10⁵ cells/mL in RPMI containing serial dilutions of the test drugs. Cell viability was determined after 96 h at 37 °C by the 3-(4,5-dimethylthiazol-2-yl)-2,5-diphenyltetrazolium bromide (MTT) method. Activity against solid-tumor-derived cells was evaluated in exponentially growing cultures seeded at 5 × 10⁴ cells/mL and allowed to adhere for 16 h to culture plates before addition of the drugs. Cell viability was determined by the MTT method 4 days later.

Linear Regression Analysis. Tumor cell growth at each drug concentration was expressed as a percentage of untreated controls, and the concentration resulting in 50% (IC₅₀) growth inhibition was determined by linear regression analysis.

Acknowledgment. The authors thank the Centro Interdipartimentale di Metodologie Chimico-Fisiche and the Centro Interdipartimentale di Analisi Strumentale dell'Università di Napoli "Federico II". This work was supported by a grant from Ministero dell'Università e della Ricerca Scientifica.

References

- Morton, R. A., Ed. *Biochemistry of Quinones*; Academic Press: New York, 1965.
- Wakelin, L. P. G.; Waring, M. J. DNA Intercalating Agents. In *Comprehensive Medicinal Chemistry*; Sammes, P. G., Ed.; Pergamon Press: Oxford, U.K., 1990; Vol. 2, pp 703–724.
- Chabner, B. A.; Allegra, C. J.; Curt, G. A.; Calabresi, P. Antineoplastic Agents. In *Goodman and Gilman's The Pharmacological Basis of Therapeutics*, 9th ed.; Hardman, J. G., Limbird, L. E., Molinoff, P. B., Ruddon, R. W., Gilman, A. G., Eds.; McGraw-Hill: New York, 1996; pp 1233–1287.
- Lown, J. W. *Anthracycline and Anthracenedione-Based Anticancer Agents*; Elsevier: Amsterdam, 1988.
- Carter, S. K.; Crooke, S. T. *Mitomycin C: Current Status and New Developments*; Academic Press: New York, 1979.
- Rao, K. V.; Cullen, W. P. Streptonigrin, an Antitumor Substance. I. Isolation and Characterization. *Antibiot. Ann.* **1959**, 950–953.
- Liquori, A. M.; DeLerma, B.; Ascoli, F.; Transciatti, M. Interaction between DNA and polycyclic aromatic hydrocarbons. *J. Mol. Biol.* **1962**, *5*, 521–526.
- Miller, E. C.; Miller, J. A. Mechanisms of chemical carcinogenesis. *Cancer* **1981**, *47*, 1055–1064.

- (9) Bolognese, A.; Correale, G.; Manfra, M.; Lavecchia, A.; Mazzoni, O.; Novellino, E.; Barone, V.; Pani, A.; Tramontano, E.; La Colla, P.; Murgioni, C.; Serra, I.; Setzu, G.; Loddo, R. Antitumor Agents. 1. Synthesis, Biological Evaluation, and Molecular Modeling of 5H-pyrido[3,2-a]phenoxazin-5-one, a Compound with Potent Antiproliferative Activity. *J. Med. Chem.* **2001**, *45*, 5205–5216.
- (10) Bolognese, A.; Parrilli, M. ¹H and ¹³C Chemical Shift Data of Some Ommochrome Models: Substituted Benzo[3,2-a]-5H-phenoxazin-5-one. *Heterocycles* **1992**, *34*, 1829–1833.
- (11) Nan'ya, S.; Maekawa, E.; Hayakawa, H.; Kitaguchi, Y.; Ueno, Y. Synthesis of 5H-Pyrido[2,3-a]phenoxazin-5-one and 5H-Pyrido[3,2-a]phenoxazin-5-one Derivatives. *J. Heterocycl. Chem.* **1985**, *22*, 1483–1885.
- (12) Barret, R.; Daudon, M. Synthesis of Quinonimines with Iodoxybenzene. *Synth. Commun.* **1990**, *20*, 1543–1549.
- (13) Fleming, I. *Frontier Orbitals and Organic Chemical Reactions*; John Wiley & Sons: Chichester, U.K. 1976.
- (14) Frisch, M. J.; Trucks, G. W.; Schlegel, H. B.; Scuseria, G. E.; Robb, M. A.; Cheeseman, J. R.; Zakrzewski, V. G.; Montgomery, J. A., Jr.; Stratmann, R. E.; Burant, J. C.; Dapprich, S.; Millam, J. M.; Daniels, A. D.; Kudin, K. N.; Strain, M. C.; Farkas, O.; Tomasi, J.; Barone, V.; Mennucci, B.; Cossi, M.; Adamo, C.; Jaramillo, J.; Cammi, R.; Pomelli, C.; Ochterski, J.; Petersson, G. A.; Ayala, P. Y.; Morokuma, K.; Malick, D. K.; Rabuck, A. D.; Raghavachari, K.; Foresman, J. B.; Ortiz, J. V.; Cui, Q.; Baboul, A. G.; Clifford, S.; Cioslowski, J.; Stefanov, B. B.; Liu, G.; Liashenko, A.; Piskorz, P.; Komaromi, I.; Gomperts, R.; Martin, R. L.; Fox, D. J.; Keith, T.; Al-Laham, M. A.; Peng, C. Y.; Nanayakkara, A.; Challacombe, M.; Gill, P. M. W.; Johnson, B.; Chen, W.; Wong, M. W.; Andres, J. L.; Gonzalez, C.; Head-Gordon, M.; Replogle, E. S.; Pople, J. A. *Gaussian 99*, Development Version, revision C.01; Gaussian, Inc.: Pittsburgh, PA, 2000.
- (15) Adamo, C.; Barone, V. Toward Reliable Density Functional without Adjustable Parameters: The PBE0 Model. *J. Chem. Phys.* **1999**, *110*, 6158–6170.
- (16) Adamo, C.; Cossi, M.; Barone, V. An Accurate Density Functional Method for the Study of Magnetic Properties. The PBE0 Model. *THEOCHEM* **1999**, *493*, 145–157.
- (17) Foresman, J. B.; Frisch, M. *Exploring Chemistry with Electronic Structure Methods*, 2nd ed.; Gaussian Inc., Pittsburgh, PA, 1998.
- (18) Adamo, C.; Cossi, M.; Rega, N.; Barone, V. In *New Computational Strategies for the Quantum Mechanical Study of Biological Systems in Condensed Phases, in Theoretical Biochemistry Processes and Properties of Biological Systems, Theoretical and Computational Chemistry*; Eriksson, L. A., Ed.; Elsevier Science B. D.: New York, 2001; Vol. 9, pp 467–538.
- (19) Martin R. B. In *Metal Ions in Biological Systems*; Sigel, H., Ed.; Dekker: New York, 1985; Vol. 19.
- (20) Nakazawa, H.; Chou, F. E.; Andrews, P. A.; Bachur, N. R. Chemical Reduction of Actinomycin D and Phenoxazine Analogues to Free Radicals. *J. Org. Chem.* **1981**, *46*, 1493–1496.

JM020918W